Table II were obtained by adding 90% of the ZPE to the MP2//RHF/CEP-21G* energies of the individual species.[21] As can be be seen from Table II, at all the levels of calculations examined, Cl stabilization of a vinylic moiety is larger than that of Br by ca. 1.3 kcal mol^{-1}.

The similarity between the observed 1.5 kcal mol^{-1} $\Delta G°$ value[13] and the calculated (isolated molecule) difference in double-bond stabilization energies by bromine and chlorine is remarkable. The important consequence of the greater double-bond stabilization by Cl is that the reactivity of the vinyl chloride may be reduced by up to ca. 10-fold compared with the vinyl bromide. Since the observed element effect in many cases is actually close to unity, a compensating effect, reducing the relative reactivity of the vinyl bromide, has to exist. Several causes are possible: (a) The transition state leading to the carbanion 1, X = C, is stabilized better with X = Cl than with X = Br. A recent calculation of the negative hyperconjugative abilities of the two halogens in carbanions CH_2CH_2X showed somewhat higher stabilization of chlorine than of bromine.[22a] If this also applies for the total stabilization of 1, and for the transition state leading to it, then preferential Cl stabilization should decrease the k_{Br}/k_{Cl} value.[22b] (b) The larger bulk of bromine should result in a larger steric hindrance to approach of a nucleophile to the double bond, as found for other bulky substituents.[10] This factor, which was observed in the k_{Br}/k_{Cl} ratio for nucleophilic attack on halo bicyclo[1.1.0]butanes[23] should also reduce the k_{Br}/k_{Cl} ratios. (c) β-Electron-withdrawing substituents may reduce the differential double-bond stabilization as is the case with the β-ethoxy group.[15] However, these groups should enhance the XC=C resonance interaction in contrast to the ether functionality. These three possible causes may compensate for the ground-state stabilization effect, bringing the k_{Br}/k_{Cl} ratios to near unity.

Double bond stabilization by the halogens should be important in other types of reactions of vinyl halides. A literature search for radical additions to vinyl chlorides and bromides gave no relevant data. The k_{Br}/k_{Cl} ratios of 0.23 and 0.46 for the electrophilic addition of CF_3COOH to 2-halopropenes[24a] and for the acetolysis of α-halo-*p*-methoxystyrene[24b] are dominated by stabilization of the transition state for α-halocarbocation formation by the halogen.

The most important consequence of our result is for cases where the k_{Br}/k_{Cl} value is appreciably higher than unity. In reactions proceeding by nucleophilic addition, these cases would have been regarded as authentic examples of either a stepwise mechanism (eq 1, route a) with k_2 rate determining or a single-step substitution (eq 1, route b). Our theoretical calculations, which corroborate Hine's data, suggest that such interpretation of the data could be erroneous. That is, $k_{Br}/k_{Cl} > 1$ can be obtained even when route a with k_1 being the rate-determining step is the operative mechanism. In this case the element effect will reflect the greater loss of ground-state stabilization for the vinyl chloride than for the vinyl bromide rather than involvement of C-X bond cleavage at the transition state.[25]

Registry No. CH_3Cl, 74-87-3; CH_3Br, 74-83-9; CH_4, 74-82-8; H_2C=$CHBr$, 593-60-2; H_2C=CH_2, 74-85-1; H_2C=$CHCl$, 75-01-4; Br, 7726-95-6; Cl, 7782-50-5.

(21) Hehre, W. H.; Radom, L.; Schleyer, P. v. R.; Pople, J. A. *Ab initio Molecular Orbital Theory*; Wiley: New York, 1986.

(22) (a) Data for Cl: Apeloig, Y.; Karni, M.; Rappoport, Z. *J. Am. Chem. Soc.* **1983**, *105*, 2784. Rappoport, Z.; Avramovitch, B.; Karni, M.; Apeloig, Y. *Isr. J. Chem.* **1988**, *29*, 267. Data for Br: Apeloig, Y.; Karni, M.; Rappoport, Z., unpublished results. (b) However, due to certain assumptions in the calculations and the small differences between Cl and Br, this should be regarded as an auxiliary rather than a main argument.

(23) Hoz, S.; Aurbach, D. *J. Am. Chem. Soc.* **1983**, *105*, 7685.

(24) (a) Peterson, P. E.; Bopp, R. I. *J. Am. Chem. Soc.* **1967**, *89*, 1283. Peterson, P. E.; Bopp, R. I.; Ajo, M. M. *Ibid.* **1970**, *92*, 2834. (b) Rappoport, Z.; Gal, A. *J. Chem. Soc., Perkin Trans. 2* **1973**, 301.

(25) A referee commented that likewise it would seem that a k_{Br}/k_{Cl} ratio of ca. unity is no longer firm evidence for route a.

Substituent Effects on the Geometry of the Cyclooctatetraene Ring

Carl Trindle*

Chemistry Department, University of Virginia, Charlottesville, Virginia 22903

Troy Wolfskill

Chemistry Department, Lycoming College, Williamsport, Pennsylvania 17701

Received January 23, 1991

Cyclooctatetraene can achieve a variety of geometries, tub, crown, chaise, and octagonal or distorted planar forms, depending on the system's charge and spin multiplicity. Our ab initio computations, which produce optimum geometries, relative energetics, and vibrational frequencies, provide a coherent story of the influences of charge and spin, consistent with a Walsh analysis. Since acceptor and donor substituents may alter the net charge on a cyclooctatetraene ring, such substituents might affect the geometry of the ring. We used the AM1 model for the wave function and electronic energy to evaluate the impact of substituents on charge distribution in the ring and on the inversion barrier. Qualitative perturbation molecular orbital analysis suggests that substituents would force charge alternation in the ring, reduce bond length alternation, and lower the inversion barrier. These predictions were borne out for a model donor ($-CH_2$ anion) and a model acceptor ($-CH_2$ cation). However, more easily accessible substituents, the donor methoxy and the acceptor formyl, had minor effects on the inversion barrier. Multiple acceptor or donor substitution and push-pull substituents exaggerated the charge alternation, but had little impact on inversion barriers. Fused-ring derivatives, such as the biscyclopentacyclooctatetraenes, suffered less of the bias arising from σ-system strain toward a puckered singlet cyclooctatetraene ring, and in these systems electron donors were particularly effective in flattening the ring.

The cyclooctatetraene (COT) ring can take on a number of forms, which we characterize as crown, chaise, tub, and plane (Figure 1). The planar ring can be a regular octagon or take on a 4-fold symmetry. We report calculations on various ions of the hydrocarbon ring, substituted forms of the neutral ring, and fused-ring systems that bear on the

0022-3263/91/1956-5426$02.50/0

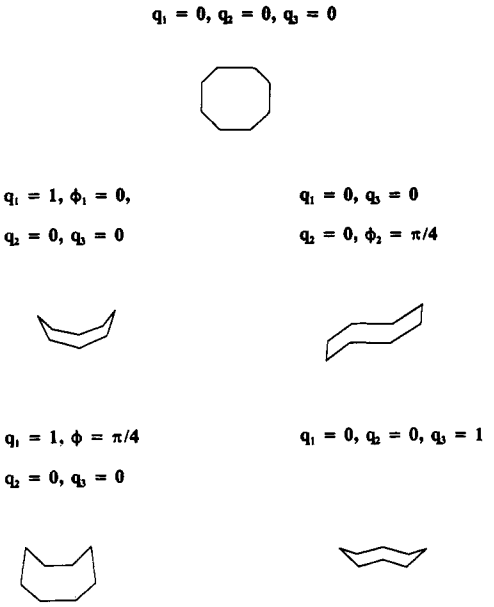

Figure 1. Structures of the eight-membered ring, with Cremer–Pople puckering coordinates. The coordinates q_1, q_2, and q_3 correspond to formation of tub, chaise, and crown, respectively. The angles ϕ correspond to pseudorotation coordinates.

questions of the preferred structure of the hydrocarbon ring as the number and orbital assignment of π electrons in the system changes and under what circumstances might the ring be flattened. We make a number of suggestions that might aid the synthesis of planar neutral COT ring systems.

Data Bearing on the Structures of the Ions of Cyclooctatetraene

Cyclooctatetraene has inspired a great deal of experimental and theoretical study since its synthesis by Willstätter[1] in 1911. The neutral ground-state ring takes on a "tub" shape of symmetry D_{2d}.[2] The unsubstituted dication has not been observed, but proton NMR studies suggest that substituted forms of the dication are planar and aromatic.[3] NMR evidence[4,5] also suggests that the dianion is aromatic with D_{8h} symmetry, the form it assumes in many metal complexes. X-ray studies indicate that the 8-fold rotation symmetry may be reduced in the dianion by crystal-packing asymmetries[6-8] though planarity is maintained. A chaise geometry is seen in single crystals of $COT[Fe(CO)_3]_2$.[9]

The D_{8h} forms of the COT monoanion and monocation are both subject to Jahn–Teller distortion. Shida and Iwata[10] report the electronic spectrum for COT monocation and suggest that the ring is puckered (D_{2d} symmetry). Data on the COT monoanion, including NMR[4,5,11,12] and electronic spectra[10,13,14] can be interpreted on the alternative assumption that the distortions from D_{8h} symmetry are negligible. Vibronic modeling of EPR spectra led McLachlan and Snyder[15] to propose a D_{4h} geometry with alternating C–C bond lengths of 1.41 and 1.36 Å. Recent MCD studies[16] suggest departures from D_{8h} symmetry, though the nature of the distortion (to planar D_{4h} or to puckered D_{2d} symmetry) has not been established. We are not aware of any experimental evidence for the structures of the neutral open-shell singlet or triplet.

Table I. Electronic Configurations and States for D_{8h} COT

charge	configuration	state	predicted structure
+2	$(a_{1u})^2(e_{1g})^4$	$^1A_{1g}$	D_{8h}
+1	$(a_{1u})^2(e_{1g})^4(e_{2u})^1$	$^2E_{2u}$	D_{4h} or D_{2d} (JT active in D_{8h})
+0	$(a_{1u})^2(e_{1g})^4(e_{2u})^2$	$^1A_{1g}$	D_{2d} closed-shell singlet
+0	$(a_{1u})^2(e_{1g})^4(e_{2u})^2$	$^1B_{1g}$	D_{2d} closed-shell singlet
+0	$(a_{1u})^2(e_{1g})^4(e_{2u})^2$	$^1B_{2g}$	D_{8h} open-shell singlet
+0	$(a_{1u})^2(e_{1g})^4(e_{2u})^2$	$^3A_{2g}$	D_{8h} open-shell triplet
−1	$(a_{1u})^2(e_{1g})^4(e_{2u})^3$	$^2E_{2u}$	D_{4h} or D_{2d} (JT active in D_{8h})
−2	$(a_{1u})^2(e_{1g})^4(e_{2u})^4$	$^1A_{1g}$	D_{8h}

Semiempirical MINDO/2 calculations, parametrized to produce structures and energetics in organic molecules,[17] are consistent with the experimentally suggested structures for the neutral singlet (D_{2d}), dianion, and dication (D_{8h}). The monocation is predicted to have a puckered D_{2d} structure. While MINDO/2 calculations produce a D_{2d} structure for the monoanion, a similar scheme with improved parametrization, MNDO,[18] predicts a planar D_{4h} structure.[19] MINDO/2[20] and MNDO[21] calculations of the neutral D_{8h} triplet indicate that it is aromatic and less stable than the D_{8h} singlet, apparently violating Hund's rule.

Many details of the structures of COT species remain to be established, particularly for the open-shell neutral and singly charged species. Here, we report ab initio SCF studies employing split valence basis sets to calculate optimized geometries for COT species containing 6–10 π electrons. We established the nature of extreme points by calculations of the curvature matrix and vibrational frequencies in the STO-3G basis. The results of these calculations are rationalized, at least in broad outline, by qualitative bonding theory.

Walsh Analysis of Cyclooctatetraene Geometry

Walsh[22] developed a pictorial analysis of variations of orbital energies with nuclear distortions that allowed the prediction of geometries for a variety of molecules. The analysis begins with the nuclei in a high-symmetry arrangement and an initial ordering of molecular orbitals by energy. The response of each orbital's energy to a normal mode distortion is then judged pictorially. A molecular orbital will be stabilized if bonding atomic orbitals (amplitudes in-phase) are brought closer together by the distortion or if antibonding atomic orbitals (amplitudes out-of-phase) are separated. Conversely, the molecular

(1) Willstätter, R.; Waser, E. *Dtsch. Chem. Gest.* **1911**, *44*, 3423.
(2) Basteansen, O.; Hedberg, L.; Hedberg, K. *J. Chem. Phys.* **1957**, *27*, 1311.
(3) Olah, G. A.; Staral, J. S.; Liang, G.; Paquette, L. A.; Melega, W. P.; Carmody, M. J.; *J. Am. Chem. Soc.* **1977**, *99*, 3349.
(4) Katz, T. J. *J. Am. Chem. Soc.* **1960**, *82*, 3784.
(5) Katz, T. J.; Strauss, H. L. *J. Chem. Phys.* **1960**, *32*, 1873.
(6) Goldberg, S. Z.; Raymond, K. N.; Harman, C. A.; Templeton, D. H. *J. Am. Chem. Soc.* **1974**, *96*, 1348.
(7) Noordik, J. H.; van den Hark, T. E. M.; Mooij, J. J.; Klaassen, A. A. K. *Acta Crystallogr., Sect. B* **1974**, *30*, 833.
(8) Noordik, J. H.; Degens, H. M. L.; Mooij, J. J. *Acta Crystallogr., Sect. B* **1975**, *31*, 2144.
(9) Dickens, B.; Lipscomb, W. N. *J. Am. Chem. Soc.* **1961**, *83*, 489.
(10) Shida, T.; Iwata, S. *J. Am. Chem. Soc.* **1973**, *95*, 3473.
(11) Strauss, H. L.; Katz, T. J.; Fraenkel, G. K. *J. Am. Chem. Soc.* **1963**, *85*, 2360.
(12) Jones, M. T.; de Boer, E. *Mol. Phys.* **1982**, *47*, 487.
(13) Kimmel, P. I.; Strauss, H. L. *J. Phys. Chem.* **1968**, *72*, 2813.
(14) Dvorak, V.; Michl, J. *J. Am. Chem. Soc.* **1976**, *98*, 1080.
(15) McLachlan, A. D.; Snyder, L. C. *J. Chem. Phys.* **1962**, *36*, 1159.
(16) Samet, C. Ph. D. Dissertation, University of Virginia, 1988.
(17) Dewar, M. J. S.; Harget, A.; Haselbach, E. *J. Am. Chem. Soc.* **1969**, *91*, 7521.
(18) Dewar, M. J. S.; Gleicher, G. J. *J. Am. Chem. Soc.* **1965**, *87*, 685.
(19) Glidewell, C.; Lloyd, D. *Tetrahedron* **1984**, *40*, 4455.
(20) Baird, N. C. *J. Am. Chem. Soc.* **1972**, *94*, 4941–4948.
(21) Dewar, M. J. S.; Merz, K. M., Jr. *J. Chem. Soc., Chem. Commun.* **1985**, 343.
(22) Walsh, A. D. *J. Chem. Soc.* **1953**, 2260.

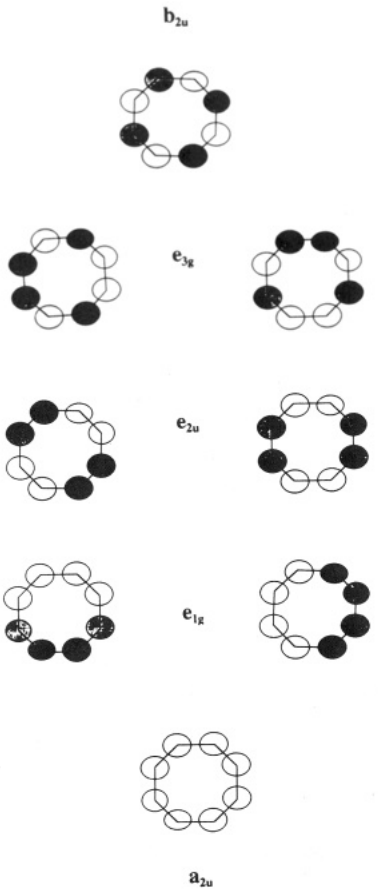

Figure 2. π MO's for COT in D_{8h} symmetry. Note that the orbitals within degenerate sets can be mixed freely, retaining degeneracy and completeness (see Figure 7)

orbital is destabilized if bonding atomic orbitals are separated or antibonding atomic orbitals are brought together. These effects can usually be judged by inspection and correspond to first-order perturbations, the perturbation operator being the distortion, which is totally symmetric in the symmetry to which it leads the molecule. This work has since been extended, in particular by Gimarc.[23]

The closed-shell singlet states for the D_{8h} system are multiconfigurational; the labels in Table I refer to the D_{4h}-distorted states, which are more adequately represented by single configurations.

It should be noted that the Walsh analysis neglects the energetics of the σ frame, which always favors a puckered geometry in order to minimize CCC angle strain. A planar conformation should then only be assumed if it is unequivocally favored by the π system.

The π MO's for COT in D_{8h} symmetry are displayed in Figure 2. The low-lying electronic configurations and states that arise from the assignment of 6–10 electrons to these MO's are presented in Table I, with Walsh predictions for their geometries. We will give particular attention to the in-phane b_{2g} mode, leading to D_{4h} symmetry, and the following out-of-plane modes: the e_{2u} mode, which produces the D_{2d} tub, the e_{3g} mode, which produces the chaise, and the b_{1u} mode, which leads to the crown. These four ring-puckering modes are displayed in Figure 3.

A reviewer has pointed out that the b_{1g} in-plane deformation, which produces alternating bond angle increases and decreases, meets the group-theoretic criterion for a Jahn–Teller active mode. Inspection of the e_{2u} orbitals

(23) Gimarc, B. M. *Molecular Structure and Bonding: the Qualitative Molecular Orbital Approach*; Academic: New York, 1979.

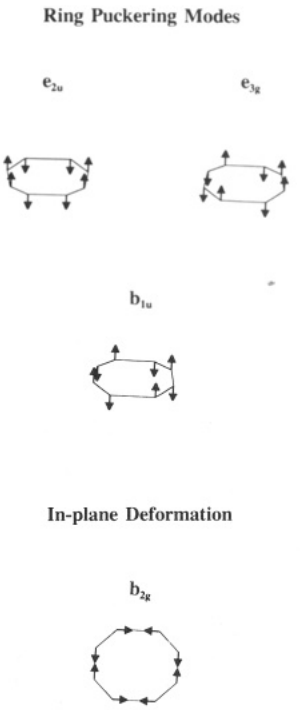

Figure 3. Ring deformation leading to bond length alternation, and the ring puckering modes for COT within the D_{8h} point group. Absent members of degenerate pairs may be obtained by a rotation of $\pi/4$ radians.

suggests that this motion would not produce significant splitting (symmetry-allowed mixing is not always strong). The deformation would also be opposed by the σ framework. There is no experimental suggestion that the b_{1g} distortion is as stabilizing as the b_{2g} deformation considered here.

Figure 4a shows the response of Walsh orbitals to the b_{2g} in-plane deformation, leading to a D_{4h} symmetry with alternating bond lengths. The MO's favor this distortion for all species with the exception of the dianion, dication, and open-shell neutral states. We thus expect bond alternation to occur in the closed-shell neutral species as well as the monocation and monoanion.

Figure 4b shows the response of MO's to the e_{2u} (tub) puckering, which destabilizes the lowest lying a_{2u} MO (not shown), thus favoring the planar form of the dication. Upon puckering the e_{2u} MO is split and MO occupation will govern the preferred geometry. The A_1 cation will strike a balance between the destabilization of the two electrons in the lowest lying level (not shown) and the stabilization of the single electron in the a_1 level. The neutral closed-shell species, with two electrons in the a_1 level, will most strongly favor this distortion. The open-shell neutral species are not stabilized by this mode, with the influence of the a_1 and a_2 electrons canceling, and the π system should favor the planar form. The monoanion experiences a net effect much like the monocation, and the extent of its puckering will be determined by a balance of opposing forces. The dianion is stable in the planar octagonal geometry.

Figure 4c presents the effects of an e_{3g} chaise distortion on the π MO's. The picture is much the same as for the e_{2u} distortion, except that the e_{1g} level is destabilized. The neutral closed-shell singlet will have two electrons in the stabilized b_g MO and should thus be the least resistant to chair deformations. An equilibrium chaise geometry is not predicted, however.

The b_{1u} crown distortion, shown in Figure 4d, retains the degeneracy of the e_{2u} HOMO–LUMO pair. The a_{2u}

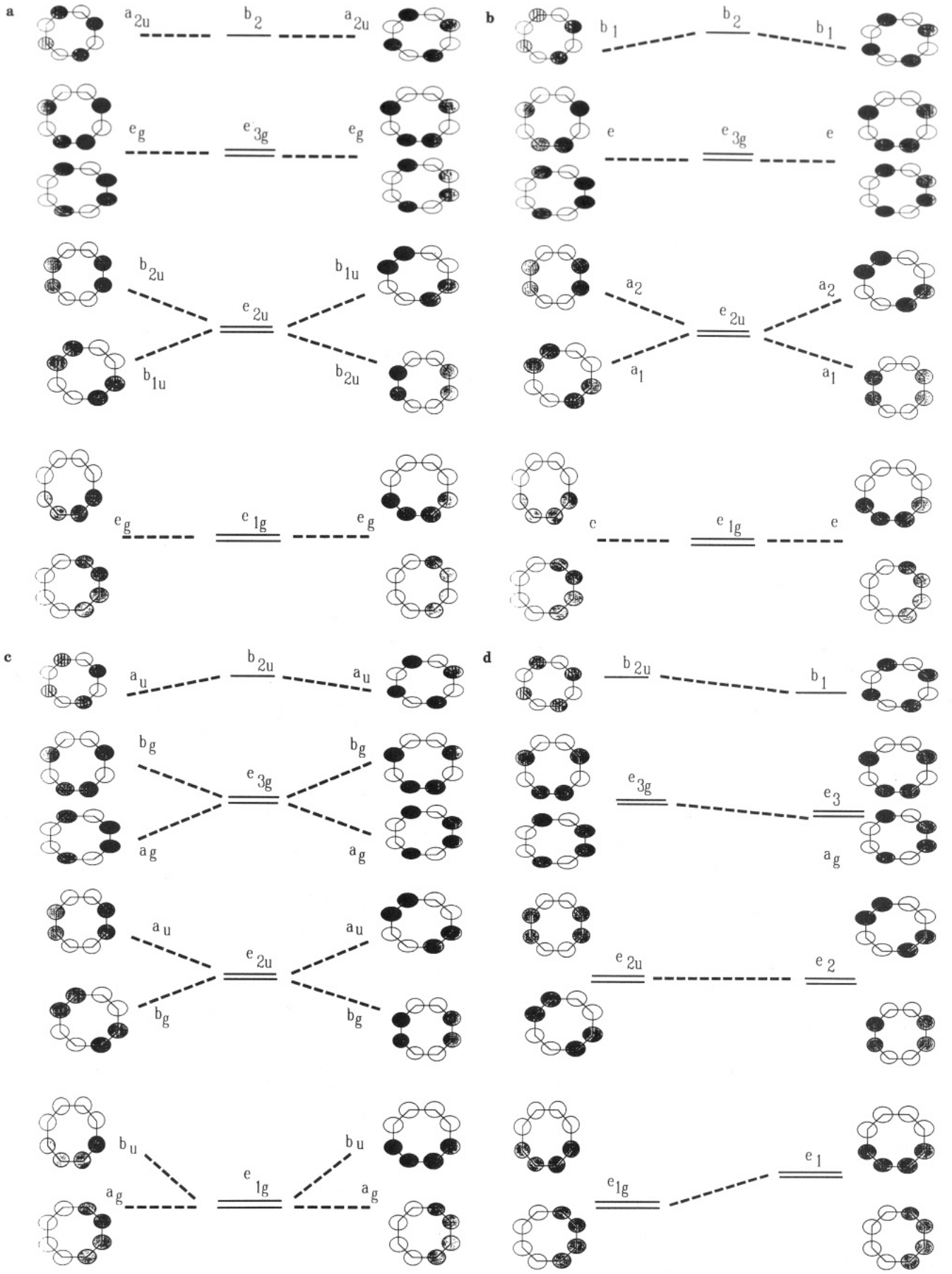

Figure 4. Walsh diagrams for the effect on π MO energies due to various distortions of the octagonal-planar cyclooctatetraene ring. The lowest energy a_{2u} π MO opposes all distortions and is not shown. A. The response of Walsh orbitals to the b_{2g} in-plane deformation, leading to a D_{4h} symmetry with alternating bond lengths. B. The response of MO's to the e_{2u} (tub) puckering. C. The response of MO's to the e_{3g} (chaise) distortion. D. The response of MO's to the b_{1u} (crown) distortion.

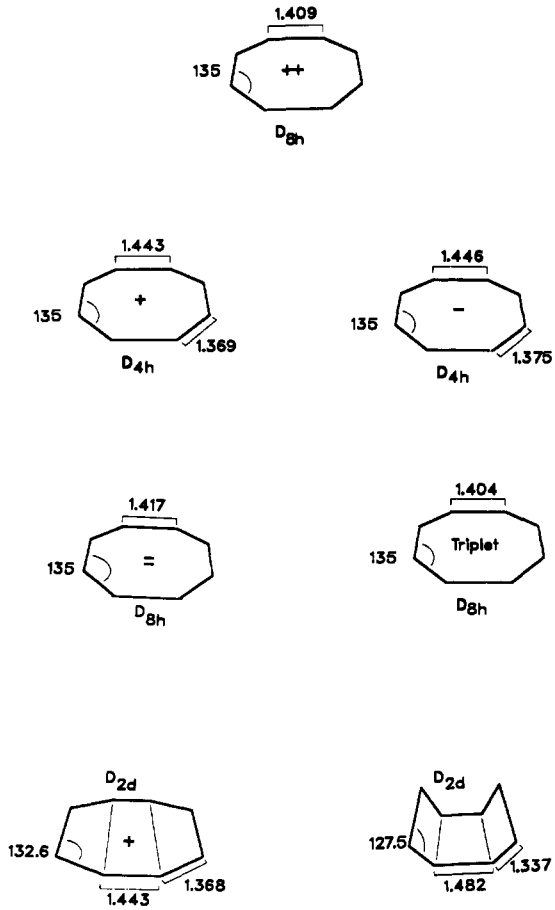

Figure 5. Optimized geometries for COT species obtained with a double-ζ basis for the valence orbitals (DZV basis).

and e_{1g} levels are both destabilized, so no stable crown geometry is anticipated.

Computational Methods

We used the HONDO-7 system[24] operating on the University of Virginia IBM 3090 computer for ab initio calculations. Geometries were optimized to gradients of 0.015 milliHartrees per Bohr. Standard basis sets in HONDO-7 were used throughout. Both restricted open-shell Hartree–Fock (ROHF) and unrestricted Hartree–Fock (UHF) optimizations were performed for high spin states. Attempts to include polarization were unsuccessful due to the limited disk space available. Attempts to calculate two-configuration MCSCF wave functions for the neutral D_{8h} closed-shell species were unsuccessful for the same reason.

We use MOPAC 4.00[25] running on the University of Virginia IBM 3090 for semiempirical calculations. All calculations were performed using the AM1 Hamiltonian and the Precise option to tighten convergence tolerances.

We describe puckering with the help of Pople–Cremer coordinates.[26] These coordinates are a finite Fourier transform of displacements of the ring atoms from a mean plane. For the eight-membered ring there are puckering coordinates q_1 corresponding to puckering toward the D_{2d} tub; q_2 corresponding to puckering toward the chaise; and q_3, corresponding to puckering toward the crown. All distortions but q_3 have a phase angle, ϕ, which changes

(24) Dupuis, M.; Watts, J. D.; Villar, H. O.; Hurst, G. J. B. HONDO: Ab Initio HFMO Calculations (Version 7.0), QCPE no. 544.
(25) Stewart, J. J. P. MOPAC: A General Molecular Orbital Package. Version 5.0, QCPE no. 455.
(26) Cremer, D.; Pople, J. A. *J. Am. Chem. Soc.* **1975**, *97*, 1354.

Table II. STO-3G Frequencies for Ring Puckering Modes of COT Species[a]

				frequencies (cm^{-1})				
sym	chg	spin	wfn	e_{2u}	e_{2u}	e_{3g}	e_{3g}	b_{1u}
D_{8h}	+2	1	RHF	98	98	414	414	664
D_{2d}	+1	2	ROHF	94	209	442	442	696
D_{4h}	+1	2	UHF	63*i*	198	442	442	688
D_{4h}	+1	2	ROHF	57*i*	199	448	448	696
D_{2d}	0	1	RHF	196	288	465	465	787
D_{4h}	0	1	RHF	148*i*	255	429	429	742
D_{8h}	0	3	UHF	181	181	509	509	651
D_{4h}	-1	2	UHF	149	254	535	535	681
D_{4h}	-1	2	ROHF	150	256	538	538	688
D_{8h}	-2	1	RHF	251	251	576	576	633

[a] Definitions: sym = symmetry series; chg = charge; wfn = form of wave function.

value during pseudorotation. Note that mode q_1 interconverts one tub-puckered structure (with $\phi_1 = \pi/4$) to an equivalent tub structure (with $\phi_1 = -\pi/4$) by pseudorotation through the structure with $\phi = 0$. The total puckering amplitude, or the sum of squares of displacements from the mean plane is given by Q, where $Q^2 = \Sigma_j q_j^2$. The relation between puckering coordinates and more vivid shape names is illustrated in Figure 1.

Computational Results on the Structures of Cyclooctatetraene Ions

Figure 5 shows optimized geometries for COT species obtained with a double-ζ basis for the valence orbitals (DZV basis).[24,27] The puckering amplitudes may be more sensitive to the quality of the basis than are the other geometric parameters. Lacking polarization functions in the basis, we view these values as approximations. For open-shell species UHF and ROHF values for geometric parameters are in excellent agreement, with minor deviations (<0.01 Å) being found in puckering amplitudes. Semiempirical results are in general agreement with ab initio values.

The ab initio optimized geometries present a convincing illustration of the predictive value of the Walsh analysis. The dication, dianion, and open-shell neutral species display rigid octagonal forms with C–C bond lengths of about 1.40 Å. The monocation, monoanion, and closed-shell neutral species all show strong bond alternation around the 1.40-Å average bond length common to all species. Bond lengths were about 1.33 and 1.48 Å for the neutral species and 1.36 and 1.44 Å for the monoions. Puckering is most pronounced in the neutral closed-shell ring (1.1 Å). This is reduced in the monocation (0.6 Å), while the monoanion is computed to be planar.

Ab initio C–C bond lengths tend to be overestimated, while C=C and C–H bond lengths tend to be underestimated in the DZV basis. AM1 bond lengths are competitive with ab initio calculations and improve on them in many instances, though the C–H bond lengths are somewhat overestimated.

AM1 results suggest a slight (0.002 Å) D_{2d} distortion for the monanion, while ab initio calculations indicate a planar D_{4h} geometry. (While the AM1 puckering seems negligible, the planar form does have an imaginary frequency.) AM1 and ab initio results are in substantially better agreement for the monoanion than reported MINDO/2 calculations.[17]

As the Walsh analysis suggested, crown and chaise distortions are opposed in all species. The ordering of resistance to puckering from optimized planar geometries

(27) Hehre, W. J.; Radom, L.; Schleyer, P. v. R.; Pople, J. A. *Ab Initio Molecular Orbital Theory*; Wiley-Interscience: New York, 1986.

Table III. Puckering Amplitudes and Inversion Barriers for COT Ions

species	q_1(tub); ϕ_1	q_2(chair); ϕ_2	q_3(crown)	$\Delta H^{\ddagger}_{inversion}$ (kcal/mol)	model
COT	1.115; 45.0	0.0; 0.0	0.0	12.1	AM1
	1.118; 45.0	0.0; 0.0	0.0	11.0	STO-3G
	1.064; 45.0	0.0; 0.0	0.0	12.4	DZV
COT cation	0.736; 45.0	0.0; 0.0	0.0	2.6	AM1
	0.483; 45.0	0.0; 0.0	0.0	0.5	STO-3G[a]
	0.594; 45.0	0.0; 0.0	0.0	0.9	DZV[a]
COT anion	0.144; 0.0	0.0; 0.0	0.0	0.0	AM1
	0.000; 0.0	0.0; 0.0	0.0	0.0	ab initio

[a] Restricted open-shell formalism; unrestricted formalism produces barriers of 0.3 (STO-3G) and 1.4 kcal/mol (DZV).

is also well-characterized, with crown puckering being the most strongly opposed and tub puckering being the easiest according to the STO-3G frequencies displayed in Table II. The monocation and neutral singlet are stabilized by tub puckering, according to the imaginary frequencies for that mode in the planar species. Increasing negative charge stiffens the tub mode.

It is well-known that single-determinant calculations with the STO-3G basis do not represent vibrational frequencies accurately. However, there is a strong correlation between frequencies computed in this way and observed frequencies; scaling the computed frequencies by a factor of about 0.83 often produces reliable frequencies (±40) cm^{-1}). DZV frequencies are more accurate; scaling by a factor of about 0.90 products realistic (±40 cm^{-1}) frequencies.[27] Even after scaling some vibrational frequencies are not accurately described; multiconfigurational effects or (equivalently) unconventional bonding is often suggested in such cases.

To summarize: ab initio calculations of the optimized structures of various COT species are consistent with the experimental conclusions for the structures of the neutral singlet (puckered D_{2d}) and dication and dianion (octagonal D_{8h}). The hypothesis of a D_{2d} geometry for the monocation, used to interpret electronic absorption data, is supported as well, in agreement with previous semiempirical calculations. In contrast to semiempirical calculations for the monoanion, which predict a slight D_{2d} distortion, we compute a minimum energy D_{4h} structure with about a 150 cm^{-1} frequency potential opposing D_{2d} puckering distortions.

The barrier for inversion of the neutral cyclooctatetraene ring through a D_{4h} transition state is strikingly reduced by the removal or addition of charge, as Table III makes clear. The AM1 ring inversion barrier of 12.1 kcal/mol computed for neutral unsubstituted COT is in reasonable agreement with the generally quoted experimental value of 13.7 kcal/mol.[28,29] This compares well with other reported values: molecular mechanics[30] estimates 15.1 kcal/mol, while MINDO/2 predicts 17 kcal/mol.[17] A minimal basis ab initio calculation[31] produces a barrier of 17.8 kcal/mol, while our DZV calculation gives 12.4 kcal/mol. AM1 and ab initio computational models agree that the barrier is reduced by almost a power of 10 for the cation, while the anion prefers the planar geometry.

Studies of the Inversion Barrier in Neutral Singlet COT

NMR evidence[32,33] suggests that conformational inversion from tub to tub may occur via the two pathways illustrated in Figure 6. The first path involves a simple inversion through a D_{4h} planar intermediate. The second path involves shifting from alternating bond structures through a suggested D_{8h} form. Either of these processes can lead to the interconversion of isomers for substituted species.[34] Substituents tend to raise the barriers, which is attributed to steric effects. Stable bond shift isomers have been synthesized.[29] No experimental studies of the inversion barriers for the ions of COT have been reported.

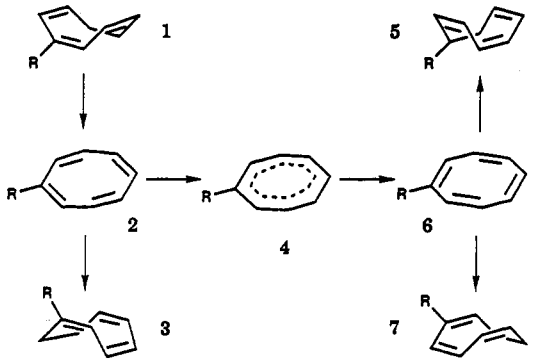

Figure 6. Pathways for conformational inversion from tub to tub according to NMR data.[27,28] The planar species with alternating C–C bond distances is a transition state for inversion, but (for that very reason) cannot be the transition state for valence tautomerization.

Computational studies of the cyclooctatetraene ring inversion barrier[17,30] and the bond shift barrier[35] have been reported; these affirm the proposed inversion pathways. While steric effects on the ring inversion barrier have been studied,[29] to our knowledge no systematic treatment of substituent electronic effects on ring geometry and inversion barriers has been reported.

AM1 Studies of Substituent Effects on Puckering Amplitudes and Ring Inversion Barriers in Cyclooctatetraene Derivatives

Puckering amplitudes for cyclooctatetraene vary over a wide range as electrons are added to or subtracted from the π MOs of the ring. In this section we report the results of application of Dewar's AM1 parametrization of the SCF-MO scheme to investigate the effects of electron donation and withdrawal by substituents on the geometry and inversion barrier of neutral COT. We have computed the AM1-optimized geometries for both puckered and planar forms of a variety of substituted and fused ring COT derivatives. We were guided in these studies by the following qualitative considerations.

(28) Anet, F. A. L. *J. Am. Chem. Soc.* **1962**, *84*, 671.
(29) Anet, F. A. L.; Bourn, A. J. R.; Lin, Y. S. *J. Am. Chem. Soc.* **1964**, *86*, 3576.
(30) Allinger, N. L; Sprague, J. T.; Finder, C. J. *Tetrahedron* **1973**, *29*, 2519.
(31) Wipff, G.; Wahlgren, U.; Kochanski, E.; Lehn, J. M. *Chem. Phys. Lett.* **1971**, *11*, 350.
(32) Anet, F. A. L.; Bock, L. A. *J. Am. Chem. Soc.* **1968**, *90*, 7130.
(33) Naor, R.; Luz, Z. *J. Chem. Phys.* **1982**, *76*, 5662.
(34) Paquette, L. A. *Pure Appl. Chem.* **1982**, *54*, 987.
(35) Dewar, M. J. S.; Merz, K. M., Jr. *J. Phys. Chem.* **1985**, *89*, 4739.

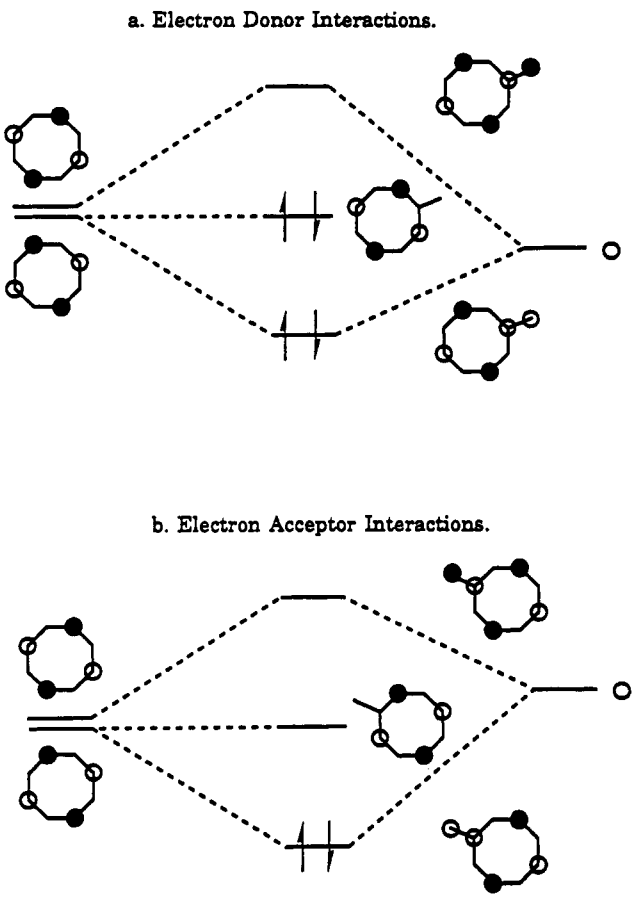

Figure 7. A. Donor effects: electron density is depleted at the site of attack, COT's LUMO is destabilized, and the HOMO of the substituent is stabilized. B. Acceptor effects: electron density is enhanced at the site of substitution, the substituent's LUMO is destabilized, and COT's HOMO is stabilized.

Figure 7 illustrates the MO interactions that are anticipated when an electron donor or acceptor approaches COT in a hypothetical D_{8h} geometry. An electron acceptor will be characterized by a low-lying LUMO that can mix with the HOMO of COT. Approach of the substituent should polarize the e_{2u} π MO's of COT so to maximize the acceptor-ring interaction. Consequently, charge alternation should appear in the ring, with electron density being accumulated at the site of attack. Bond formation then stabilizes the HOMO of COT and destabilizes the LUMO of the substituent; electron density is withdrawn from the ring. This should reduce the puckering amplitude as in COT cation. If the polarization is of sufficient magnitude, the bond alternation may be reduced.

A donor will be characterized by a HOMO that can interact with the COT LUMO. Similar effects, also described in Figure 7, accompany bond formation, though now electron density is depleted at the site of attack, COT's LUMO is destabilized, and the HOMO of the substituent is stabilized. Electron density is donated into the ring and should lead to ring flattening as in COT anion. The complementary nature of attack by donors and acceptors suggests that the effects may be maximized by 1-donor-4-acceptor substitution, leading to a push–pull mechanism in which total charge transfer with the ring may be reduced while charge alternation should be increased.

We chose formyl [-CHO] as the model π acceptor and methoxy [-OMe] as the model π donor and investigated monosubstituted and multiply substituted species. These included multiple donors, multiple acceptors, and donor–acceptor pairs. The monosubstituted species at least should be easy targets for the synthetic chemist.

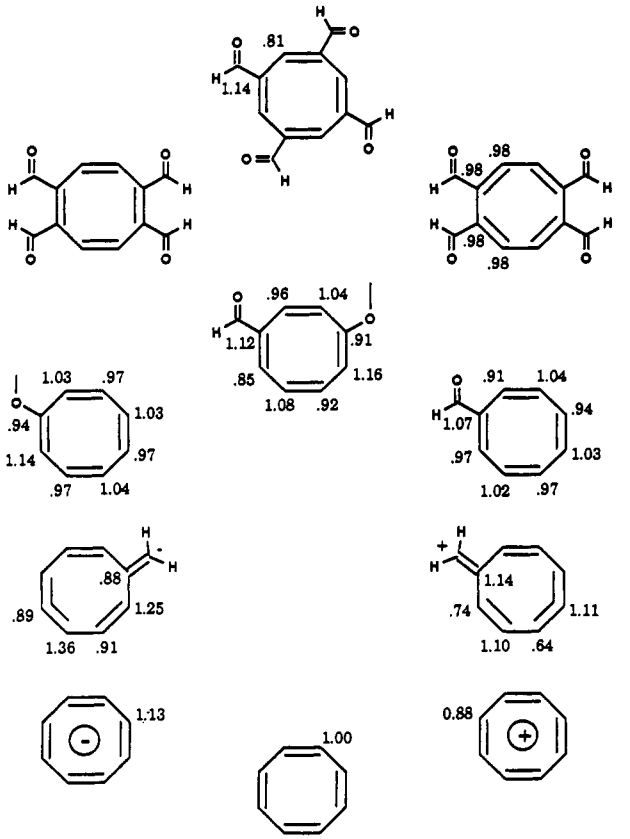

Figure 8. AM1 charges for ring π orbitals for planar conformations of substituted cyclooctatetraenes. Values are not reported for planar 1,2,5,6-tetramethoxy-COT, which is neither an equilibrium nor a transition-state structure.

Computational Method for Substituted Cyclooctatetraenes

All our calculations on substituted cyclooctatetraenes employed the AM1 Hamiltonian as realized in MOPAC 5.00[36] running on a microVAX at Lycoming College. Both puckered and planar geometries were optimized for all species using the Precise option to tighten the SCF and gradient convergence criteria. The large fused ring species were difficult to optimize, however, and the tighter gradient convergence criteria were not satisfied in all cases. Gradient norms for the reported geometries are at most ca. 0.5 kcal/Å. The nature of all extreme points, as minima or saddle points, was ascertained via frequency calculations for all optimized geometries. Out-of-plane distortions are reported in terms of Cremer–Pople puckering coordinates[26] with q_1, q_2, and q_3 corresponding to puckering toward the tub, chaise, and crown, respectively.

Computational Results

I. Charge Alternation in Planar COT Geometries. AM1 atomic π charges for the COT ring carbon atoms are shown in Figure 8. Neutral D_{4h} COT has a total of eight π electrons in the eight-carbon ring. Methylene-ion substitution provides an extreme case of charge flow, with the anion donating 0.82 electrons to the π system and the cation withdrawing 0.78 electrons. In contrast, single methoxy and formuyl substituents interact weakly with the π network; methoxy donates 0.09 π electrons, while

(36) Stewart, J. J. P. MOPAC: A General Molecular Orbital Package. Version 5.0, QCPE no. 455.

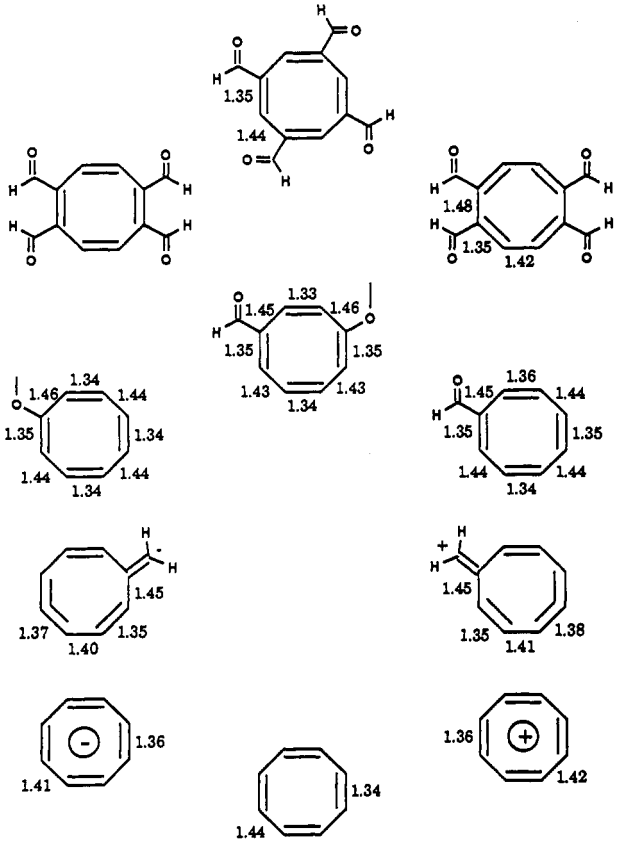

Figure 9. Ring carbon–carbon bond lengths found in planar conformations of substituted cyclooctatetraenes. Values are not reported for planar 1,2,5,6-tetramethoxy-COT, which is neither an equilibrium nor a transition-state structure.

formyl withdraws 0.04 electrons. Multiple substitution by methoxy leads to fairly strong interactions, however; 0.41 electrons are donated to the ring by the 1,3,5,7-tetramethoxy substitution, while 0.31 electrons are donated to the ring in the 1,2,5,6-arrangement. However, the fact that the planar tetramethoxy species is not an equilibrium geometry casts doubt on the estimate of charge transfer. The tetraformyl substitution withdraws 0.19 and 0.13 electrons from the ring. Push–pull 1-donor-4-acceptor substitution leads to both increased charge alternation and decreased total charge transfer, as seen in the entries for 1-methoxy-4-formylcyclooctatetraene.

II. Bond Length Alternation in Planar Geometries. Carbon–carbon bond length alternation as found in planar conformations is illustrated in Figure 9. The optimized D_{4h} geometry of COT shows alternating C–C bond lengths of 1.44 and 1.34 Å, giving mean deviations of 0.05 Å from the average. This is reduced in both the monoanion and monocation, with mean deviations near 0.03 Å.

Substitution by methylene ions changes the alternation pattern, since a C_{2h} symmetry is found for the planar geometry. All other substituted and fused ring species maintain strong bond alternation, though small modifications of the COT bond lengths are seen. In particular, we note that for singly substituted species both single and double bonds adjacent to the substitution site are lengthened while remote sites are barely affected. This is true for 1-methoxy-4-formyl-COT as well, though now the C2–C3 double bond is shortened.

III. Puckering Coordinates and Ring Inversion Barriers. AM1 puckering coordinates for substituted COT species are presented in Table IV. Heats of formation and ring inversion barriers are listed in Table V. The AM1 method represents the geometry of COT ions

Table IV. Puckering Coordinates for Substituted COT Species[a]

	q_1(tub); ϕ_1	q_2(chair); ϕ_2	q_3(crown)
	Donor		
methylene anion	0.592; 90.00	0.242; 45.0	−0.106
methoxy-	1.118; 45.11	0.004; −41.42	0.003
1,3,5,7-tetramethoxy-	1.136; 45.60	0.000; 0.000	0.000
1,2,5,6-tetramethoxy-	1.128; 45.00	0.000; 0.000	0.000
	1.205; 45.00	0.000; 0.000	0.003
	Acceptor		
methylene cation	0.841; −90.00	0.315; 45.00	−0.126
formyl-	1.126; 45.12	0.001; −47.27	0.000
1,3,5,7-tetraformyl-	1.137; 46.16	0.000; 0.00	0.000
1,2,5,6-tetraformyl-	1.172; 45.00	0.000; 0.00	0.000
	1.196; 45.00	0.000; 0.00	0.006
	Mixed Substituent Species		
1-methoxy-4-formyl-	1.127; 45.1	0.007; −44.5	0.005

[a] q's in angstroms; ϕ's in degrees.

Table V. AM1 Heats of Formation and Inversion Barriers for Substituted COT Species

species	$\Delta H_{puckered}$	ΔH_{planar}	$\Delta H^{\ddagger}_{inversion}$
COT neutral	63.5	75.6	12.1
COT cation	249.2	251.8	2.6
	Donor-Substituted Species		
methylene anion	53.9	56.7	2.8
methoxy-	26.5	37.9	11.4
	Acceptor-Substituted Species		
methylene cation	250.4	261.0	10.5
formyl-	33.7	46.7	13.1
1,3,5,7-tetraformyl-	−55.0	−39.7	15.3
1,2,5,6-tetraformyl-	−47.8	−16.2	31.6
	Mixed-Substituent Species		
1-MeO-4-formyl-	−3.8	8.2	12.1

reasonably well; the AM1 value of the q_1 (tub) puckering amplitude, 1.12 Å, is a useful reference. Puckering amplitudes of 0.74 for COT cation and 0.0 for COT anion suggest that electron donors will be more effective than electron acceptors in modifying the ring geometry.

Reported ring inversion barriers are the difference between the heats of formation for the puckered and planar forms of the ring, the geometries independently optimized.

$$\Delta H^{\ddagger}_{inversion} = \Delta H_{planar} - \Delta H_{puckered}$$

For the extreme cases of substitution by positive and negative methylene, tub puckering is reduced to 0.84 Å in the cation and 0.59 Å in the anion. (Considerable admixture of the chaise distortion is seen, however, reflecting the lowered symmetry and local flattening.) The inversion barrier is reduced in both cases, as well, to 10.5 and 2.8 kcal/mol for the cation and anion, respectively. The larger perturbations accompanying substitution by methylene anion are consistent with the larger perturbations in COT anion relative to COT cation.

More conventional substitution seems to make little impact on the extent of puckering. Contrary to our expectations, methoxy and formyl substituents have little effect on the puckering amplitude. Multiple substitution, either at the 1,3,5,7 or 1,2,5,6 positions, yields minor changes for the puckering. For the multiply substituted formyl species, the inversion barrier is substantially raised, presumably through steric interactions. Push–pull 1-methoxy-4-formyl substitution, which we anticipated would maximize the effects of substitutions, is seen to have little effect on the puckering amplitude, leaving the inversion barrier the same as in parent COT. Inversion barriers for the multiply substituted methoxy species are

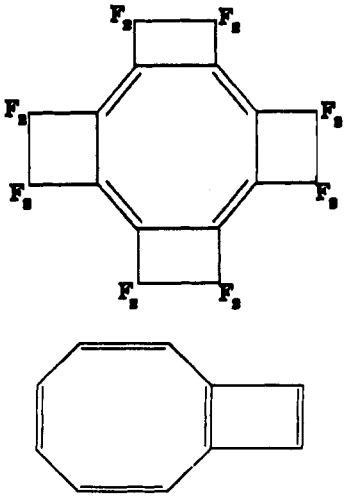

Figure 10. Planar structures of ring-fused bicyclo[6.2.0]decapentaene[30] and tetrakis(perfluoro)cyclobutyl-COT,[31] according to X-ray studies.

not reported. The calculation of the inversion barrier requires that we find a transition state, characterized by an imaginary frequency for one normal mode, which leads to the puckered geometry. The planar multiply substituted methoxy species, for which the methoxy groups were coplanar with the ring, showed several imaginary frequencies, however, and thus did not correspond to a transition state. The planar forms for all other molecules do correspond to transition states.

Flattening Cyclooctatetraenes

We have not managed to induce flattening of the COT ring by substituent electronic effects, even in the extreme cases of substitution by methylene ions. Substituents that flatten the COT ring have been identified, though the flattening does not appear to involve electronic effects. X-ray studies of the ring fused bicyclo[6.2.0]decapentaene[37] and tetrakis(perfluoro)cyclobutyl-COT,[38] illustrated in Figure 10, reveal both to be planar. While the Hückel rule might suggest that the decapentaene would be aromatic, alternating bond lengths are found. MMP2 calculations led Allinger and Yuh[39] to propose that the bicyclodecapentaene ring is antiaromatic, with σ strain being the source of ring flattening. This appears to be the case for the cyclobutyl-fused molecule as well, according to AM1 semiempirical calculations of the cyclobutyl and cyclbuteno-fused COT species.[40,41]

We have investigated a variety of fused-ring derivatives of COT, displayed in Figure 11, modeling the energy and geometry with the AM1 Hamiltonian. The consistent performance of the AM1 Hamiltonian in the description of the parent COT and its ions reassures us that the AM1 parametrization is entirely adequate for the discussion of the charge, geometry, and energetics of these large but analogous systems. For all bis ring-fused species, two bond shift isomers are considered, one in which the fused ring spans a C–C double bond of the eight-membered ring, and another in which the fused ring spans a C–C single bond in the ring. In order to differentiate these isomers we will refer to the former as the D isomer, for double bond spanning, and the latter as the S isomer, for single bond spanning.

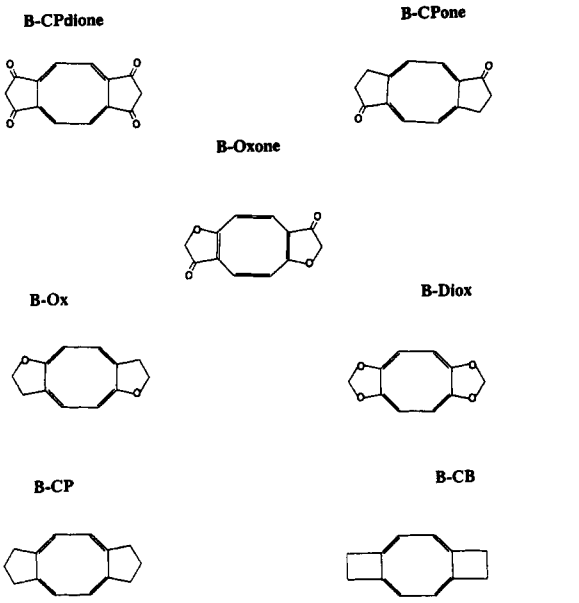

Figure 11. Fused-ring derivatives of COT for which we report AM1 energies and geometries. Abbreviations: bis-cyclopentadiona-COT = B-CPdione; bis-cyclopentanona-COT = B-CPone; bis-oxalono-COT = B-Oxone; bis-oxolana-COT = B-Ox; bis-dioxalano-COT = B-Diox; bis-cyclopenta-COT = B-CP; bis-cyclobuta-COT = B-CB.

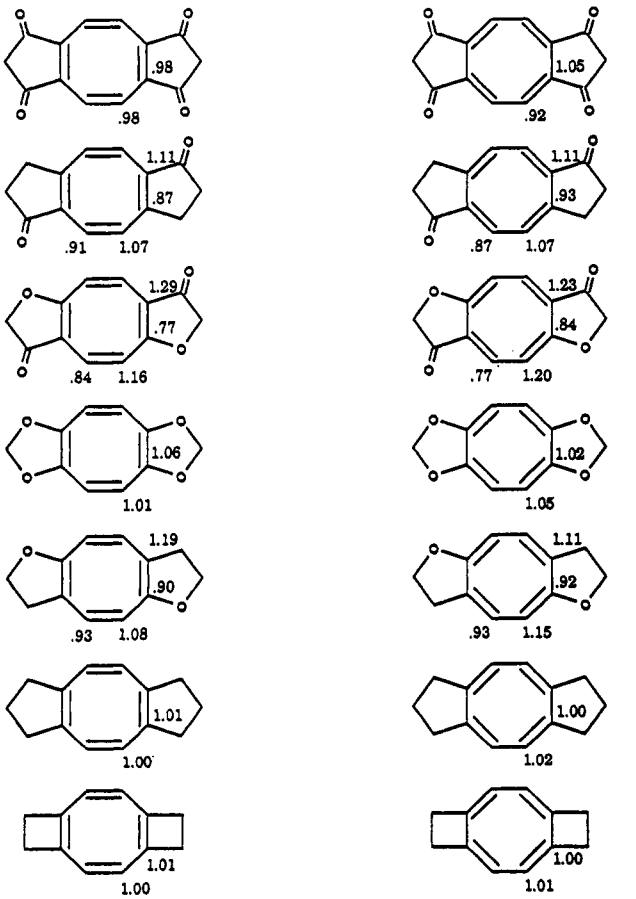

Figure 12. AM1 charges for ring π orbitals in fused-ring-substituted cyclooctatetraenes.

Hydrocarbon ring fusion leads to charge transfer similar in magnitude to that seen in the singly substituted species. The incorporation of donors and acceptors in the fused ring magnifies this effect, as shown in Figure 12. Ether oxygens

(37) Kabuto, C.; Oda, M. *Tetrahedron Lett.* **1980**, 103.
(38) Einstein, F. W. B.; Willis, A. C.; Cullen, W. R.; Soulen, R. L. *J. Chem. Soc. Chem. Commun.* **1981**, 526.
(39) Allinger, N. L.; Yuh, Y. H. *Pure Appl. Chem.* **1983**, *55*, 191.
(40) Mak, T. C. W.; Li, W.-K. *THEOCHEM* **1982**, *89*, 281.
(41) Li, Y.; Rubin, Y.; Diederich, F.; Houk, K. N. *J. Am. Chem. Soc.* **1990**, *112*, 1618.

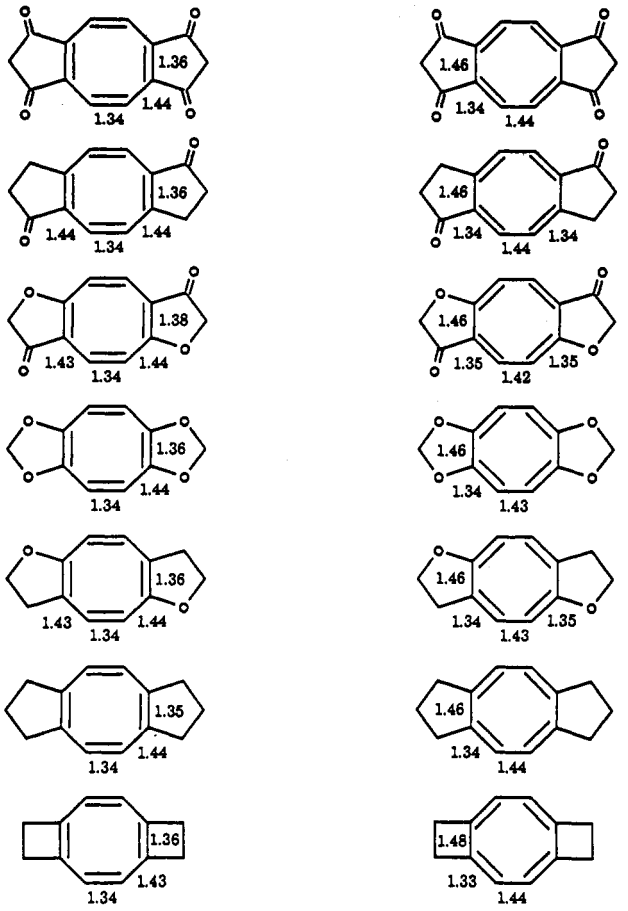

Figure 13. COT ring carbon–carbon bond lengths found in planar conformations of ring-fused derivatives of cyclooctatetraene.

produce the largest charge flow seen in the fused rings, bis-oxalano donating 0.20 electrons and bis-dioxalano donating 0.26 or 0.29 electrons. Again 1-donor-4-acceptor substitution as found in the bis-oxolanone species increases the charge alternation and decreases the total charge flow.

Ring fusion leads to lengthening of the COT bond to which the rings are fused in all cases. For five-membered ring fused species, the magnitude of the expansion is constant with the exception of bis-oxalanona (D) COT, for which a push mechanism may be operating to lengthen the COT fused bond to a greater extent. In bis-cyclobuta-COT, a slight contraction of the bonds adjacent to the fusion site is also seen. This bond length shortening is not evident in the five-membered fused hydrocarbon ring species. Thus, the nonfused COT bonds will display electronic effects, if any, of substitution on bond length alternation in the ring. For all molecules that include ether oxygens in the fused rings, no systematic or dramatic expansion of ring double bonds and contraction of ring single bonds is evident. Figure 13 displays bond lengths for the eight-membered ring for bis-fused species. The predicted reduction of bond alternation is not borne out for these species.

Puckering amplitudes for a variety of fused-ring COT derivatives are presented in Table VI. Heats of formation, ring inversion barriers, and enthalpy changes for bond shift isomerization for all bis fused rings are presented in Table VII. The fused-ring systems display smaller puckering amplitudes and inversion barriers relative to the parent or simply substituted systems. Any molecular model kit provides a convenient mechanical model for ring flattening in these species. Constructing COT from standard sp^2 carbon atoms yields a D_{2d} tub geometry. If the hydrogens

Table VI. Puckering Amplitudes for Bis-Fused-Ring Substituted COT Species

species	spans	q_1(tub); ϕ_1	q_2(chair); ϕ_2	q_3(crown)
B-CB	D	0.515; 45.0	0.0; 0.0	0.0
	S	0.000	0.0	0.0
B-CP	D	0.984; 45.0	0.0; 0.0	0.0
	S	0.759; 43.5	0.0; 0.0	0.0
		Donor Ring Substituents		
B-Ox	D	0.867; 44.1	0.0; 1.0[a]	0.0
	S	0.553; 46.0	0.0; 0.0	0.0
B-Diox	D	0.587; 45.0	0.0; 0.0	0.0
	S	0.000	0.0	0.0
		Acceptor Ring Substituents		
B-CPone	D	0.969; 44.8	0.0; −23.8[a]	0.0
	S	0.019; −49.5	0.0; −44.8[a]	0.0
		Mixed Ring Substituents		
B-CPdione	D	0.944; 45.0	0.0; 0.0	0.0
	S	0.758; 43.5	0.0; 0.2[a]	0.0
B-Oxone	D	0.816; 44.8	0.0; 0.0	0.0
	S	0.008	0.0	20.0

[a] Very small puckering amplitude in this mode. The pahse angle, though defined, has little significance. D and S refer to isomers in which a double or single bond of the COT ring is spanned by the fused-ring substituent. Amplitudes q reported in angstroms, phase angles ϕ in degrees.

Table VII. AM1 Heats of Formation, Ring Inversion Barriers, and Bond Shift Isomer Enthalpy Differences for Bis-Fused-Ring Derivatives of COT[a]

species	isomer	ΔH_fplanar	ΔH_fequil	$\Delta H^{\ddagger}_{\text{inversion}}$	$\Delta H^{\ddagger}_{\text{bondshift}}$
B-CB	D	120.1	120.7	0.5	
	S	105.1	105.1	0.0	−15.1
B-CP	D	41.5	50.2	8.7	
	S	43.4	48.6	5.1	+1.9
B-Ox	D	−8.9	−4.3	4.6	
	S	−7.2	−6.3	0.9	+1.7
B-Diox	D	−64.1	−63.2	0.9	
	S	−68.4	−68.4	0.0	−4.3
B-CPone	D	−7.3	+0.2	7.5	
	S	−1.9	−1.9	0.02	+5.3
B-CPdione	D	−46.9	−40.0	6.9	
	S	−49.9	−46.4	3.5	−3.0
B-Oxone	D	−57.5	−54.8	2.8	
	S	−53.6	−53.6	0.0	+4.0

[a] Energies in kcal/mol. $\Delta H^{\ddagger}_{\text{inversion}} = \Delta H_f$planar − ΔH_fequilibrium; $\Delta H^{\ddagger}_{\text{bondshift}} = \Delta H_f$double spanning − ΔH_fsingle spanning; D and S refer to double and single bond spanning isomers, respectively. Abbreviations: bis-cyclopentadiona-COT = B-CPdione; bis-cyclopentanona-COT = B-CPone; bis-oxalono-COT = B-Oxone; bis-oxolana-COT = B-Ox; bis-dioxalano-COT = B-Diox; bis-cyclopenta-COT = B-CP; bis-cyclobuta-COT = B-CB.

spanning a carbon–carbon double bond are pressed together, the ring flattens. The lower amplitudes of all single-bond spanning isomers can be appreciated by attempting to construct this isomer while maintaining the proper double-bond orientation. Considerable flexibility is required of the model in order to accommodate the strain.

Hydrocarbon fused-ring substitutions spanning single bonds in the COT ring are more effective in flattening the COT ring than are fused-ring substitutions spanning ring double bonds. For the bis-cyclobutyl fused rings, the double-bond-spanning isomer has a tub-puckering amplitude of 0.52 Å and an inversion barrier of 0.5 kcal/mol while the single-bond-spanning isomer is planar. The cis-cyclopentyl fused rings are less effective in flattening the ring. The double-bond-spanning isomer has a tub-puckering amplitude of 0.98 Å and an inversion barrier of 8.7 kcal/mol, while the single-bond-spanning isomer has an amplitude of 0.76 Å and a barrier of 5.1 kcal/mol. These values are to be compared with the parent COT

values of puckering amplitude 1.12 Å and barrier 12.1 kcal/mol.

While conventional substitution produces only minor electronic effects on COT ring geometry and inversion barrier, inadequate to overcome the strong strain bias favoring the puckered ring, such is not the case in the fused rings. As shown in Table VI, the puckering amplitudes and inversion barriers for all substituted cyclopenta-fused species are reduced from the values computed for the parent hydrocarbon bis-cyclopentyl-fused ring. Consistent with the trends seen in COT cation and anion, acceptor (keto) substitution leads to smaller effects. Puckering amplitudes for the double-bond-spanning isomers drop from 0.98 Å in bis-cyclopentyl to 0.97 Å in bis-cyclopentanone to 0.94 Å in bis-cyclopentyl dione; the inversion barriers drop in a similar fashion from 8.7 to 7.5 to 6.9 kcal/mol. However, the single-bond-spanning isomer of the bis-cyclopentanone species has a remarkably low (0.02 Å) puckering amplitude and inversion barrier (0.02 kcal/mol). The single-bond-spanning isomer of the bis-cyclopentyl dione system in contrast, has a puckering amplitude of 0.76 Å and an inversion barrier of 3.5 kcal/mol. We observe a parallel enhancement of the charge alternation in the p atomic orbitals for the strongly flattened bis-cyclopentanone species.

Ether incorporation leads to dramatic reduction in both the out-of-plane distortions and barriers to inversion. The bis-oxalano and bis-dioxalano species show a tub-puckering amplitude for the double-bond-spanning isomer equal to 0.87 and 0.59 Å, respectively, and inversion barriers of 4.6 and 0.9 kcal/mol. The dioxalano species is thus even less distorted from the plane than COT cation. For the single-bond-spanning isomers, bis-oxalano has a tub distortion of 0.55 Å and a barrier of 0.9 kcal/mol, while the bis-dioxalano species is planar.

The bis-oxalano species is again predicted to maximize the effects via a push–pull mechanism. Its double-bond-spanning isomer has a tub-puckering amplitude of 0.82 Å and a barrier of 2.8 kcal/mol, the lowest values found with the exception of those of the bis-dioxalano species. Its single-bond-spanning isomer is planar.

Discussion and Conclusions

Our ab initio calculations on the ions of cyclooctatetraene illustrated the fact that the geometry of the COT ring is very sensitive indeed to the number of π electrons in the system and the assignment of those electrons to configurations and states. We verified that the dication, the dianion, and the neutral triplet state of COT are planar and 8-fold (D_{8h}) symmetric. The closed-shell singlet is strongly puckered to the D_{2d} tub shape. Our computations provide the strongest evidence now available that the COT cation and anion are distorted to D_{4h} by a Jahn–Teller mechanism and that the anion retains planarity while the cation is more weakly puckered than the neutral closed-shell species.

We proposed that charge effects could be induced in neutral COT derivatives by substituents and made the following predictions with the help of qualitative (PMO) theory:

(A) Donor and acceptor substituents on the COT ring will lead to charge alternation in the ring.

(B) Substituents will tend to weaken the pronounced bond length alternation in the ring.

(C) Substituents will tend to reduce the puckering amplitude of the COT ring and reduce the inversion barrier.

The predicted effects are displayed in the model methylene cation and anion substituted rings. However, more conventional substituents have little impact on ring bond lengths and do not reduce the puckering amplitude or ring inversion barrier of COT as anticipated, either alone or in concert.

Fusion of four- and five-membered hydrocarbon rings onto COT does reduce the magnitude of both the out-of-plane distortion and the barrier to planar inversion. This seems to be entirely explainable by strain effects. Substituents on the fused-ring systems have a considerable impact on the equilibrium geometries and inversion barriers. Electron donors are more effective than acceptors in flattening the ring, and push–pull mechanisms are effective as well. Planar equilibrium geometries are preferred for the single-bond-spanning isomers of bis-dioxalano- and bis-oxalono-COT, with bis-cyclopentanona-COT being nearly planar. The planar geometry of bis-dioxalano-COT is preferred over a local minimum energy puckered structure by 4.3 kcal/mol.

Planar COT species are rare; only a few cyclobuta fused ring COT species are known to be flat. The fused-ring species considered here have not to our knowledge been synthesized. We hope that the synthesis of fused-ring COT derivatives incorporating electron donors and acceptors will be pursued and that their geometry and dynamics will be determined experimentally.

Acknowledgment. Thanks to Paul Schatz and Cindy Samet for guidance, to Lester Andrews for access to the Pittsburgh Cray, to Alan Batson and Academic Computing for summer support of TAW, and to Academic Computing staff for cheerful and expert advice.